

# Theoretical Study of the Edge Effect of Dumbbell-shape Graphene Nanoribbon with a Dual Electronic Properties by First-principle Calculations

1<sup>st</sup> Qinqiang Zhang  
Dept. of Finemechanics  
Tohoku University  
Sendai, Japan

zhang.qinqiang@rift.mech.tohoku.ac.jp

2<sup>nd</sup> Takuya Kudo  
Dept. of Finemechanics  
Graduate School of Engineering  
Sendai, Japan

takuya.kudo@@rift.mech.tohoku.ac.jp

3<sup>rd</sup> Jowesh Gounder  
Dept. of Finemechanics  
Graduate School of Engineering  
Sendai, Japan

jowesh@rift.mech.tohoku.ac.jp

4<sup>th</sup> Ying Chen  
Fracture and Reliability Research  
Institute  
Tohoku University  
Sendai, Japan

ying@rift.mech.tohoku.ac.jp

5<sup>th</sup> Ken Suzuki  
Fracture and Reliability Research  
Institute  
Tohoku University  
Sendai, Japan

kn@rift.mech.tohoku.ac.jp

6<sup>th</sup> Hideo Miura  
Fracture and Reliability Research  
Institute  
Tohoku University  
Sendai, Japan

hmiura@rift.mech.tohoku.ac.jp

**Abstract**—The electronic band structure (band gap) and electronic transmission properties of dumbbell-shape graphene nanoribbons (DS-GNRs), which consists of a thinner semiconductive GNR and two wider metallic GNRs at its both ends, was theoretically investigated using first-principles calculation to clarify the dominant controlling factors of their electronic performance for their applications to various smart sensors. The electronic properties of the DS-GNR was found to vary drastically depending on the combination of the total number of carbon atoms along the width direction of each portion, the length of the semiconductive portion, the width of the metallic portion, and so on.

**Keywords**—graphene nanoribbon, dumbbell-shape structure, band gap, electronic transmission property

## I. INTRODUCTION

After the discovery of graphene in 2004, many researchers have been dedicated to explicate the basic characteristics of this outstanding material which has a great potential to substitute the conventional semiconductor material such as silicon. Previous studies have shown that a single layer of graphene sheet has been proved to show super metallic properties [1]. However, when a graphene sheet is cut into nanoscale stripe with a width thinner than 70 nm, so-called graphene nanoribbon (GNR), it starts to exhibit semiconductive properties [2], and the semiconductive properties vary a lot depending on its size. Even various graphene-based electronic applications have been proposed, however, the high performance electronic devices based on GNR have not been successfully fabricated in mass production.

It was experimentally validated that the sub-50-nm GNR showed clear semiconductive properties [3]. In addition, the semiconductive GNRs showed wide variation of the strain sensitivity of their electrical resistance under the application of uniaxial strain [4]. However, their electronic properties varied widely from metallic-like ones to semiconductive ones. There are two essential problems which caused the variation of the electrical properties. One is the periodic change in the band gap of GNRs smaller than 70 nm which appear to have a strong function of the total number of carbon atoms along the width direction of GNRs. The other is electronic junction

between the semiconductive GNR and metallic GNRs. Therefore, it is very important to control the effective band gap of the DS-GNR structure and a stable electronic junction between the semiconductive GNR and metallic GNRs.

In this study, the electronic band structure and electronic transmission properties of a novel proposed dumbbell-shape structure of GNRs were investigated by using first-principle calculations. The dumbbell-shape structure consists of different sizes of single GNRs with different edge sizes at both end portion of single GNRs. The simulation results were used for providing theoretical data and guides to fabricate highly reliable, stable and sensitive GNR-based electronic devices.

## II. ANALYTICAL MODEL OF DUMBBELL-SHAPE STURCTURE

The synthesized 40-nm wide monolayer graphene nanoribbons periodically patterned on a Si/SiO<sub>2</sub> substrate has been fabricated successfully as shown in Fig. 1 [3]. To indicate a more intuitional illustration on the simulation model of novel proposed dumbbell-shape graphene nanoribbon (DS-GNR), the structure is highlighted by blue and red color as shown in Fig. 1. The blue portions consist of the large size monolayer graphene with metallic properties, and the red ones are composed by 40-nm wide GNR stripes with semiconductive properties. The light grey areas in this figure are the deposited electrodes on the top of the DS-GNRs and the black area represents the etched area where no graphene exists on Si/SiO<sub>2</sub> substrate. It was confirmed that the DS-GNR showed semiconductive photosensitivity and the sensitivity was more than ten times higher than that of conventional silicon-base devices. However, the sensitivity of each GNR showed wide variation. Therefore, in order to fabricate highly reliable, stable and sensitive GNR-based electronic devices, a

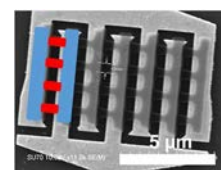


Fig. 1. GNR-based electronic device with multi-channel dumbbell-shape structure highlighted by blue and red bars. The scale is 5 micro meter.

further theoretical study is indispensable for finding out the dominant controlling factors of their electronic performance.

A simple schematic image of the developed dumbbell structure of GNR is shown in Fig. 2(a) and the simulated dumbbell-shape GNR (DS-GNR) model is also shown in Fig. 2(b). The large graphene sheet area of DS-GNR, where the graphene sheet shows metallic properties, was covered by metal electrodes. In this simulation, only the wide GNRs at both ends were considered to be electrodes. This wide GNRs with metallic properties were assumed that it had an ohmic contact with any common deposited metal electrodes, and the energy barrier between the metallic electrodes and the wide GNR was negligible. The electronic properties of a single semiconductive GNR between the two GNR electrodes are categorized into three-families:  $3p$ ,  $3p+1$ ,  $3p+2$  ( $p$  is an integer) by a total number of carbon atoms along width direction. The groups of  $3p$  and  $3p+1$  show semiconductive properties, and the group of  $3p+2$  shows semi-metallic properties as the same explanation with previous studies [5]. In this study, the  $3p+2$  type of GNR was selected as an example for representing the large area graphene/GNR which shows semi-metallic properties. The  $3p/3p+1$  types of GNR were represented for semiconductive GNRs whose width was less than or much less than 70 nm in practical application. Identically, it was regarded as narrow portion GNRs in the simulation. The model structure was assumed to be periodic along the vertical direction and has Armchair GNR (AGNR) with hydrogen termination. Hence, the pure DS-GNR has Zigzag GNR (ZGNR) with hydrogen termination perpendicular to the periodic direction. The electronic properties of pristine ZGNR and AGNR have already been studied [5]. Therefore, in this study, the electronic properties of pristine ZGNR and AGNR were recalculated as a reference to that of the novel proposed DS-GNR. However, previous studies have not shown the combined structure which has interesting electronic properties.

### III. ANALYSIS OF ELECTRONIC BAND STRUCTURE OF DS-GNR

The SIESTA package which was developed based on the density functional theory (DFT) was used for the calculations of electronic band structure in this study. The post-processing calculation was performed by using the TranSIESTA utility which was using nonequilibrium Green's function (NEGF) method based on DFT for calculating the current-voltage (I-V) characteristics of DS-GNR [6]. The generalized gradient approximation (GGA) in the Perdew-Burke-Ernzerhof (PBE) form was used to describe the exchange and correlation energy of electron-electron interactions. The conjugate gradient (CG) method was used to fully optimize all the atomic positions without any geometric constraints until the total maximum force became less than  $0.02 \text{ eV } \text{\AA}^{-1}$ . An energy mesh cutoff was set at 500 Ry. The tolerance energy of convergence was set to 0.001 eV. The k-point sampling for unit cells was constructed with a  $1 \times 20 \times 20$  Monkhorst-Pack grid. The electronic temperature was fixed at 450 K to increase the convergence speed. The vacuum area was  $10 \text{ \AA}$  on the left and right side along horizontal direction and  $7.5 \text{ \AA}$  on the top and bottom of the DS-GNR. Also, based on the frontier molecular orbital theory, the top of the valence band was also referred to as the highest occupied molecular orbitals (HOMO), and the bottom of the conduction band was referred to as the lowest unoccupied molecular orbitals (LUMO). All the orbital distribution figures shown in this study is at HOMO energy level

level since that of figures at LUMO energy level is also symmetric but shows opposite phase color.

Since it was hard to analyze the electronic properties of the actual DS-GNR structure shown in Fig.1 due to the limitation of the memory capacity of used supercomputer, a small model structure was analyzed to explicate the dominant structural factors of the dumbbell-shape structure for its electronic properties. At first, the effect of the length of the semiconductive narrow GNR on the electronic properties of the DS-GNR structure was analyzed. Because the quantum tunneling effect should appear and the electrons can jump between two wide metallic GNRs without extra energy field, when the length of narrow portion is too short.

The structures with the same width of narrow portion of DS-GNR ( $N_N = 7$ , semiconductive type) and the same width of wide portion ( $N_W = 17$ , semi-metallic type) were calculated with different length portion from  $N_L = 1$  to  $N_L = 20$ . Two examples of dumbbell-shape structures with the length portion  $N_L = 3$  and  $N_L = 7$  are shown in Fig. 3(a) on the left and right hand side, respectively. The orbital distribution of DS-GNR with  $N_L = 3$  at HOMO illustrated the quantum tunneling effect clearly. The colored area appeared throughout the whole structure. When the length of narrow portion was increased from 3 to 7, however, the localized orbital distribution started

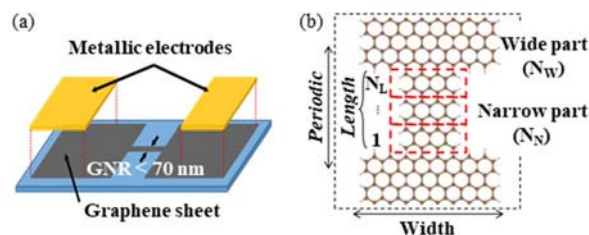


Fig. 2. (a) Simple schematic image of dumbbell-shape GNR base electronic device. (b) Simulated DS-GNR model. It consists of wide portions at both ends of narrow portion.  $N_L$  and  $N_W$  is the number of total continuous carbon atoms along the width direction.  $N_L$  is the six member ring of carbon atoms along width direction as one group which is represented by red dash line box.

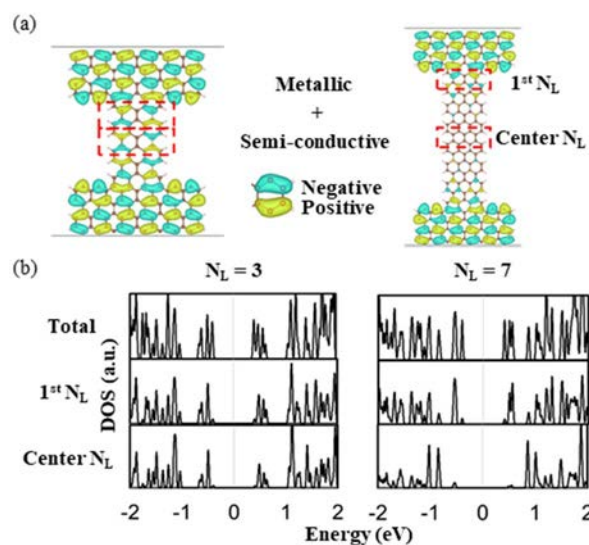


Fig. 3. (a) Simulation model with 17 at wide portion, 7 at narrow portion. Left side has  $N_L = 3$  and right side has  $N_L = 7$ . (b) Density of states of DS-GNR at different areas which are corresponding to each upper structure, respectively. Carbon atoms included in red dash line box are counted for DOS analysis.

to appear around the interface between wide portion and narrow portion. The different distributions are highlighted by red dash lines. As shown in the right hand side of Fig. 3(a), there was no orbital distribution at the center of the narrow portion. It shows the hint that when the 0 eV or higher bias voltage applied to this structure, it may show semiconductive properties which will be explained later.

The local density of states (LDOS) with different length of narrow portion of DS-GNR are shown in Fig. 3(b). The first row panel is the total density of states (DOS) of DS-GNR, and the second row panel indicates the summation of LDOS of each carbon atom included in the red-dashed box in Fig. 3(a) near the junction between wide portion and narrow portion ( $1^{\text{st}} N_L$ ). Similarly, the third row panel shows the summation of LDOS of each carbon atom exists in the red-dashed box at the center of narrow portion (center  $N_L$ ). The vertical axis of the figure is the arbitrary unit of DOS and horizontal axis is the energy. The arbitrary unit was rescaled to compare the peaks near the Fermi level. On the left side of Fig. 3(b), the LDOS doesn't show much difference among the total, first  $N_L$ , and center  $N_L$ . But the most inner peak of LDOS at center  $N_L$  with the length of narrow portion equaling 3 ( $N_L = 3$ ) was disappeared. However, on the right side of Fig. 3(b), the LDOS shows a large difference among the total, first  $N_L$  and center  $N_L$ . There were no high inner peaks around the 0.5 eV to the Fermi level which was different from the results obtained from the shorter DS-GNR. This result clearly indicates that the localized energy barriers exist in the DS-GNR.

In order to simulate the practical condition and dismiss the effect of two wide portions as described above, the length increased up to  $N_L = 20$  to find the length dependence of the narrow portion of DS-GNR. It was confirmed that the band gap increased monotonically with the length of the narrow portion as shown in Fig. 4. The band gap of DS-GNR was converged to one specific value when the length of narrow portion reached 20. Thus, the performance of the proposed DS-GNR structure is close to that of single pristine GNR when the length is long enough. This result provides the reasonable guide for experiments. As shown in Fig. 4, the curve becomes saturated when  $N_L$  is larger than 10. Since the length of carbon to carbon bonding is still around 1.42 Å after fully optimized, the width of narrow portion was about 7.2 Å and the length of narrow portion was around 42.6 Å when  $N_L = 10$ . Therefore, when the length is at least 6 times larger than the width, the performance of DS-GNR is close to that of pristine GNR at the narrow portion. This result provides the instruction to fabricate the DS-GNR for experiment that the length to width ration should be larger than 6.

Furthermore, the width dependence of DS-GNR at wide portion was also considered as edge effect. Since the wide portion should be a large graphene sheet area or GNR, the width of the wide portion was increased from 17 to 23, 29, and 41 to reach the specific value that total DOS started to show no band gap around the Fermi level. The simulated models are shown in Fig. 5(a). Two structures have the same length and width of the narrow portion which  $N_L = 7$  and  $N_N = 7$  but with different width of the wide portion which  $N_W = 17$  (left side) and  $N_W = 29$  (right side). Even when the width of the wide portion was increased to 29, the orbital distribution still showed the localized pattern. It implies the same hint of electronic transmission properties which described above. The figures of LDOS of DS-GNR are shown in Fig. 5(b). The left

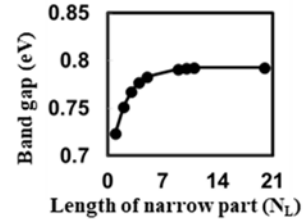


Fig. 4. Tendency of the band gap of DS-GNR with increasing length of  $N_L$

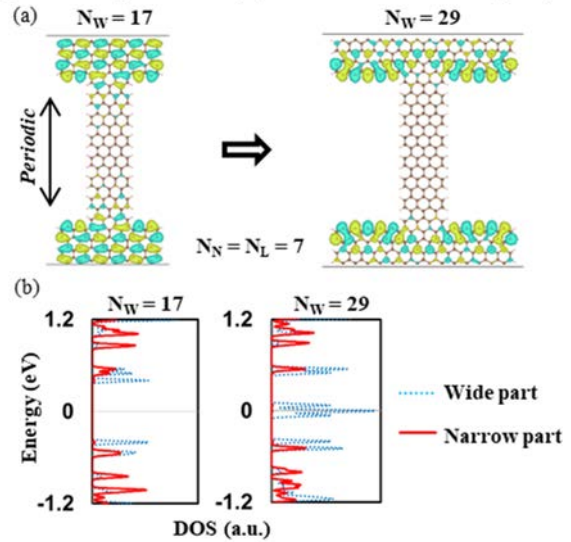


Fig. 5. (a) Simulation model with different width of wide portion. The orbital distribution of two DS-GNRs shows localized distribution. (b) Local density of states of each upper DS-GNR, respectively. Blue dashed line is the LDOS of wide portion and red line is that of narrow portion.

side is the LDOS of DS-GNR with  $N_W = 17$  and the right side is that of with  $N_W = 29$ , respectively. The vertical axis is the energy and the horizontal axis is the intensity of DOS. The blue dashed lines are the LDOS of carbon atoms in the wide portions and the red lines indicate the LDOS of carbon atoms in the narrow portion. It is clear that the band gap becomes 0 eV in the wide portion around Fermi level but the band gap does not change too much in the narrow portion. The total DOS was the summation of blue dashed and red lines, hence, the performance of the total DS-GNR structure shows metallic properties when the width of the wide portion increased to specific value, though the LDOS in the wide portion is different from that in the narrow portion. This result indicates that there exists an energy barrier around the junction area between the wide and narrow portions, even the component of this structure consists of only carbon atoms. Usually, this property appears in the structure at the boundary with different component or element. In order to further investigate the electronic properties, the post-processing was also implemented to obtain the electronic transmission properties of DS-GNR. The result is also known as the current-voltage (I-V) characteristics.

#### IV. ANALYSIS OF ELECTRONIC TRANSMISSION PROPERTIES OF DS-GNR

The schematic image of DS-GNR implemented by TranSIESTA is shown in Fig. 6(a). The scattering portion of DS-GNR was not calculated periodically in TranSIESTA, and the electrode portions were added at the both ends with periodical open boundaries. The current-voltage (I-V) curve of two structures are shown in Fig. 6(b) and Fig. 6(c), respectively. The y-axis is the current through the DS-GNR

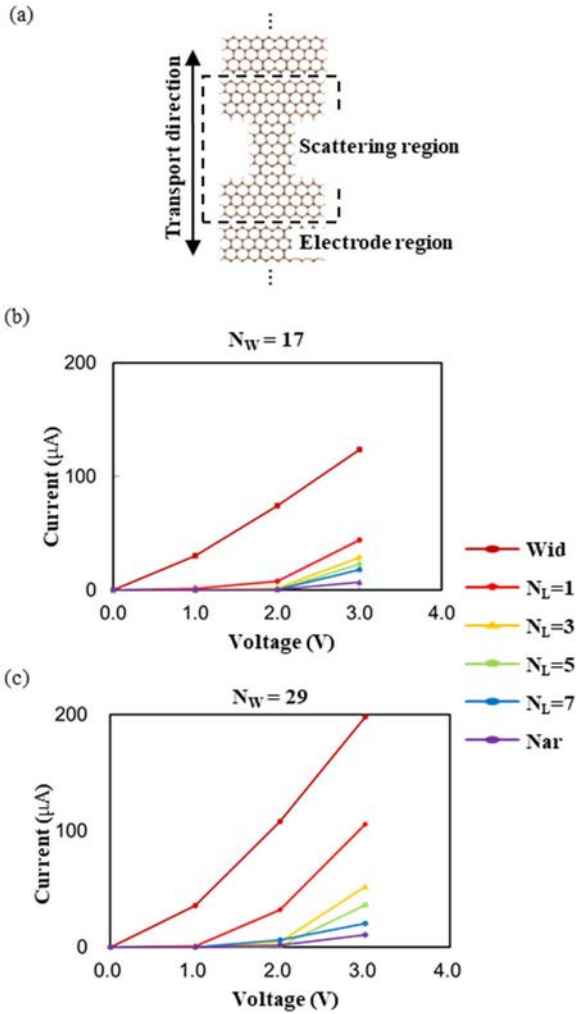


Fig. 6. (a) Schematic image of DS-GNR for electronic transmission calculation. Bias voltage applied on electrode regions and scattering region is enclosed by dash black line. (b), (c) are the current-voltage curve of DS-GNR with different length of narrow portion and that of single pristine GNR at wide and narrow portion, respectively.

along the periodical direction and the x-axis is the bias voltage applied on the structure along the periodical direction. The unit of current is micro ampere and that of voltage is volt. The line of label Wid indicates the I-V curve of pristine single GNR in the wide portion. Similarly, the line of label Nar implies the I-V curve of pristine single GNR at narrow portion.  $N_L = 1$  to 7 are the I-V curves of DS-GNR with different length of the narrow portion, respectively. Fig. 6(b) shows the tendency of I-V curve of DS-GNR with the width of wide portion 17 ( $N_W = 17$ ) and also Fig. 6(c) represents that of DS-GNR with the width of wide portion 29 ( $N_W = 29$ ). When the length of the narrow portion increased, the I-V curve became more flat due to the increase of band gap of DS-GNR. And when the length of narrow portion was long enough, the I-V curve became close to that of pristine single GNR with the same width of DS-GNR in the narrow portion.

When the width of the wide portion increased from  $N_W = 17$  to  $N_W = 29$ , however, the tendency of the length dependence didn't change too much as shown in Fig. 6(c), even when the band gap of DS-GNR with  $N_W = 29$  was zero.

Thus, the electronic transmission properties of DS-GNR was semiconductive. It also means that the localized energy barrier exists in the DS-GNR which consists of only carbon atoms. It can be explained by the LDOS of DS-GNR in the wide and narrow portions. However, the electronic transmission properties through the DS-GNR along the periodical direction have no significant relationship with the width of DS-GNR in the wide portion. The width of the wide portion of DS-GNR, therefore, doesn't affect the electronic transmission properties of DS-GNR significantly. This is because the zigzag edge effect in the wide portion of DS-GNR mainly dominates the band gap of the total system, but no significant effect on the electronic transmission properties perpendicular to the zigzag edge direction.

## V. CONCLUSIONS

In this study, the effect of the structure of DS-GNR such as the length of the semiconductive portion and the width of the wide metallic portion on its electron transmission properties was analyzed by using first principle calculation. It was found that the electronic band structure was converged to a specific value when the length of the narrow portion was at least 6 times larger than its width. Thus, the performance of the proposed dumbbell-shape structure is close to that of pristine single GNR when the length of the narrow portion is long enough. Furthermore, when the width of the wide portion is wide enough, for instance, the whole structure starts to show a localized energy barrier around the junction between the wide and narrow portions. Therefore, the electronic properties of the wide and narrow portions of DS-GNR keep their intrinsic properties even after they are jointed together. The energy barrier between them still remains even the whole structure consists of only carbon atoms. These results give basic idea of the structural design of GNR-based two dimensional electronic devices.

## ACKNOWLEDGMENT

This work was supported by JSPS KAKENHI Grant Number JP16H06357. The authors would like to express their sincere thanks to the crew of Center for Computational Materials Science of the Institute for Materials Research, Tohoku University for their continuous support of the supercomputing facilities.

## REFERENCES

- [1] Novoselov, Kostya S., et al. "Electric field effect in atomically thin carbon films." *Science* 306.5696 (2004): 666-669.
- [2] Yang, Meng, et al. " Electronic properties and strain sensitivity of CVD-grown graphene with acetylene " *Japanese Journal of Applied Physics* 55, 04EP05(2016), pp.04EP05-1~04EP05-8.
- [3] JA Goundar, et al. " Photosensitivity of Monolayer Graphene-Base Field Effect Transistor " *Proc. of ASME IMECE2019*, No. 87245, (2018), pp. 1-6.
- [4] Ryohei Nakagawa, et al. "Area-arrayed graphene nano-ribbon-base strain sensor." *Proc. of ASME IMECE2019*, No. 87277, (2018), pp. 1-6.
- [5] Son, Young-Woo, Marvin L. Cohen, and Steven G. Louie. "Energy gaps in graphene nanoribbons." *Physical review letters* 97.21 (2006): 216803.
- [6] Soler, José M., et al. "The SIESTA method for ab initio order-N materials simulation." *Journal of Physics: Condensed Matter* 14.11 (2002): 2745.